Flow–induced chain scission in dilute polymer solutions: Algorithm development and results for scission dynamics in elongational flow

H. G. Sim

Department of Energy, Environmental and Chemical Engineering, The Center for Materials Innovation Washington University, Saint Louis, Missouri 63130

B. Khomami

Department of Chemical and Biomolecular Engineering, University of Tennessee, Knoxville, Tennessee 37996

R. Sureshkumar[a)]

Department of Energy, Environmental and Chemical Engineering, The Center for Materials Innovation Washington University, Saint Louis, Missouri 63130

(Received 24 October 2006; final revision received 2 August 2007)

Synopsis

Based on covalent bond scission force estimates from single molecule experiments and a statistical analysis of the instantaneous segmental tension (ST) distribution in bead-rod chains, a new algorithm has been developed for the simulation of flow-induced polymer chain scission. This algorithm overcomes the nonphysical time-step dependence inherent in stochastic chain scission simulations that employ instantaneous ST-based criteria to identify scission events. This is accomplished by the use of a normalized ST profile that is independent of the elongation rate E for asymptotically large values of the Weissenberg number, defined as the ratio of the longest relaxation time of the chain to $1/E$. The algorithm is employed to study chain scission in steady and transient elongational flows as well as the effect of hydrodynamic interactions on chain scission in steady elongational flow. Simulation results for steady elongational flow reproduce the experimentally observed scaling law for the critical elongation rate $E_c \propto M_w^{-2}$ where M_w denotes the molecular weight. Moreover, for $E \approx E_c$, the chains unravel via a coil-to-stretch configurational transition. Since ST attains its maximum at the midpoint of the chain, the midpoint scission hypothesis (MSH) is valid. This leads to a relatively narrow distribution of daughter chains. However, for $E \gg E_c$, sufficiently large ST could develop in the elongated portions of partially coiled chains. Consequently, chain scission could occur farther from the midpoint. MSH is not valid under such conditions, and the resulting distribution of daughter chains is relatively broad. Hydrodynamic interactions are shown to slow down chain unraveling leading to an increase in E_c with the scaling $E_c \propto M_w^{-1.7}$. The effect of polymer residence time on E_c is examined by investigating scission of polymer chains that traverse the centerline of a regularized contraction flow. It is found that the scaling relationship between E_c and M_w remains the same as that for steady elongational flow given that the residence time exceeds 5% of the longest relaxation time of the chain. This result suggests that the inverse proportionality of E_c to M_w observed experimentally in contraction flow might be due to preshearing effects. Finally, the effect of loading rate on

[a)]Author to whom correspondence should be addressed; electronic mail: suresh@wustl.edu

© 2007 by The Society of Rheology, Inc.

scission probability is discussed in the context of an extended thermally activated barrier to scission model. © *2007 The Society of Rheology.* [DOI: 10.1122/1.2789945]

I. INTRODUCTION

Polymer chains can be cleaved by chemical and mechanical means. Chemical or enzymatic cleavage, such as the one employed in DNA replication (e.g., as in polymerase chain reaction), has been a subject of extensive research. Mechanically induced scission, such as the one caused by strong (extensional) flows, has also been studied experimentally since the early seventies [Horn and Merrill (1984); Keller and Odell (1985); Nguyen and Kausch (1988); Nguyen and Kausch (1990); Odell and Keller (1986); Odell *et al.* (1988); Rabin (1987); Reese and Zimm (1990); Vincent (1972)]. Experiments have also focused on chain scission in inertia-dominated and turbulent flows to understand the effects of polymer degradation on turbulent drag reduction [Choi *et al.* (2002); Lim *et al.* (2003)]. The drag reducing capability of the polymeric additives is related to the molecular extensibility [Lumley (1969); Sureshkumar *et al.* (1997)], which is proportional to the molecular weight (M_w). In turbulent flows, regions of strong, transient extensional deformation exist such as in the buffer layer between counter-rotating, quasi-streamwise vortices. Additives such as polyethylene oxide (PEO) with M_w exceeding 10^6 Da have been found to lose much of their drag reduction capability exponentially with time and within minutes after injection due to flow-induced rupture of the chains [Hunston and Zakin (1978); Matthys (1991)]. Hence, knowledge of flow-molecular configuration coupling mechanisms leading to chain scission is beneficial to drag reduction applications. In addition to skin friction control, controlled fragmentation of high M_w polymers including flexible DNA molecules is technologically relevant in the synthesis of polymers with narrow-distributed M_w and gene sequencing [Buchholz *et al.* (2004); Lengsfeld and Anchordoquy (2002); Levy *et al.* (1999)]. Flow devices such as channel/tube with abrupt contraction (with contraction ratios of order 100) have been used to achieve high throughput breakage.

The mechanism of chain scission is generally believed to be dependent on the nature of the flow. For instance, in planar extensional flows created by cross slots, opposed jets, or four-roll mills, chain breakage occurs when the strain rate exceeds a critical value that is determined by the strength of the chemical bonds between the monomers and the solvent viscosity. Under these conditions, the molecule unravels from its equilibrium, coiled state and remains in the "fully extended state" at least over a period of time comparable to the longest relaxation time $\lambda_{\max}$. The distribution of the tension in the extended chain is approximately parabolic with its maximum at the center. This has motivated statistical theoretical descriptions based on the assumption of "midpoint scission," i.e., the chain cleavage is most likely to occur at midway along the chain contour. This model leads to the prediction that the critical strain rate $E_c \propto \eta^{-1} M_w^{-2}$ where M_w is the polymer molecular weight, and η is the solvent viscosity. The above scaling for molecular weight is in good agreement with experimental observations in steady, planar extensional flows and consistent with the asymptotic behavior of a Rouse chain in elongational flow [Bird *et al.* (1987)]. Specifically, when $\lambda_H N^2 E \to \pi^2/4$, where N and λ_H denote the number of bead-spring segments and segmental relaxation time, respectively, of a Rouse chain, a coil-to-stretch configurational transition is predicted. Since $N \propto M_w$, and $\lambda_H \propto \eta$, this suggests that if the chains break in the fully extended configuration, $E_c \propto (1/\eta M_w^2)$.

By the 1980s, ample experimental evidence was provided to confirm that chain scission can also occur in Lagrangian unsteady mixed flows with elongational and shear deformation, such as the one created by the abrupt contraction flow, even if the residence

time of the polymer within the flow field is less than λ_{max}. This implies that breakage can occur even when the molecule is in a partially uncoiled state. Under such conditions, a scaling law of the form $E_c \propto M^{-1}$ where M denotes the average molar mass of the sample, which is qualitatively different from the analogous result in the case of steady elongational flow, has been obtained experimentally [Nguyen and Kausch (1988)]. Rabin (1987) rationalized the experimental observation based on slender body hydrodynamic theory. However, as pointed out by Nguyen and Kausch (1990), the hydrodynamic model predicts unrealistically low values of the maximum chain tension (up to 2 orders of magnitude lower compared to the C-C bond strength of 6–8 nN) under conditions in which chain scission is observed experimentally. Moreover, experiments using theta solvents have shown that, as in the case of steady elongation, midpoint scission is dominant in mixed flows [Nguyen and Kausch (1990)]. Midpoint scission and the relative insensitivity of polymer degradation to solvent viscosity are inconsistent with the slender body theory. Alternative explanations based on the "yo-yo" model that represents the polymer chain as two unraveling coiled ends connected by a stretched segment [Ryskin (1987)] have been proposed. However, mesoscopic simulations [Hur *et al.* (2000); Hur *et al.* (2001); Larson *et al.* (1999); Somasi *et al.* (2002)] and single molecule visualization using fluorescence microscopy [Perkins *et al.* (1997); Smith and Chu (1998); Smith *et al.* (1999)] show that the dynamics of coil-to-stretch transition, even in homogenous elongational flows, differ from those assumed in the yo-yo model. Nguyen and Kausch (1990) suggested that the inverse scaling of E_c with M and the relative insensitivity of E_c to solvent viscosity can be explained based on energetic grounds if one accounts for the internal friction (viscosity) between the segments of the coiled portions of the chain. However, their result is based on the assumption that the equilibrium statistical mechanics result for the probability of finding monomeric units close to each other holds even in presence of a transient extensional flow field. Islam *et al.* (2004) and Vanapalli *et al.* (2006) recently proposed an alternative explanation for the differences in the E_c versus M_w relationships observed in transient and steady flows based on their experimental data for the scission of PEO in aqueous-based solvents of varying viscosity in a cross-slot flow device. Specifically, these authors showed that inertia, as characterized by the Reynolds number Re based on the flow rate and slot height, has a profound impact on scission. They showed that their data as well as the literature data follow the trend $E_c \propto M^{-2}$ for $\mathrm{Re} \leqslant 1000$ whereas for $\mathrm{Re} > 1000$, $E_c \propto M^{-1}$. The change in the scaling with Re is attributed to an inertial flow transition signified by a discontinuity in the pressure drop versus the Re curve at $\mathrm{Re} \approx 1000$. These authors also showed that upon degradation, both monodispersed and polydispersed samples yielded unimodal M_w distribution for $\mathrm{Re} > 1000$ which is inconsistent with the midpoint scission hypothesis. We note that this observation is not entirely inconsistent with the previous studies since it is plausible that the flow instability threshold also corresponds to a transition point between steady ($E_c \propto M^{-2}$) and transient ($E_c \propto M^{-1}$) flows.

Theoretical modeling of mechanically induced polymer chain scission has been based on energetic considerations [Bestul (1956); Zhurkov and Korsukov (1974)]. In a broad sense, scission can be viewed as a chemical reaction. Hence, ideally, quantum mechanical level modeling is required for computing chemical bond dissociation rates in the presence or absence of external forces. However, if the flow time scale ($\sim 1/E$) is much larger than molecular vibration time scales, a coarse grained micromechanical model can be used to examine the influence of flow-induced changes in the chain conformation on scission kinetics. Moreover, if the scission threshold is determined under very small loading rate such that the activation energy for scission is not altered at the chemical bond level, it is legitimate to use this estimate in Brownian dynamics simulations (BDS) in which the

variation in segmental tension at the mesoscopic level occurs much slower than molecular time scales. Under such conditions, the applied mechanical stress is assumed to sufficiently lower the activation energy barrier for scission such that thermal fluctuations can overcome it. In a series of articles, López Cascales and García de la Torre (1991, 1992) and Knudsen *et al.* (1995, 1996) have performed BDS using bead spring models to predict chain scission in transient and steady elongational flows. In their simulations, they used linear springs (Rouse chain) as well as nonlinear Morse springs modeled by the potential $V=A(1-\exp[-B(Q-b)])^2$, where A and B are model constants (>0) and, Q and b denote the instantaneous and equilibrium lengths respectively of the spring. When $Q=b$, the spring force $F\equiv -dV/dQ=0$ whereas F reaches a maximum $F_{\max}=AB/2$ at $Q_{\max}=b+\ln 2/B$ before decaying to zero for values of $Q\gg b$. Chain scission is assumed to occur when spring potential reaches the dissociation energy ($=A$).

BDS using the above model ($N\leqslant 20$) predicts $E_c\propto(1/N^2)$ in steady elongational flow if hydrodynamic interaction (HI) between the beads is neglected, which is in excellent agreement with experiments using dilute polystyrene solution [Odell and Keller (1986)]. However, when HI is included, the exponent of N is ≈ 1.65 and 1.6 for the Rouse and Morse chains, respectively [Lopez Cascales and Garcia de la Torre (1991)]. Asymptotic analysis in the presence of HI for strong flows suggests that for a very large value of N, $E_c\propto(1/N^2\ln N)$ (as compared to $1/N^2$ in the absence of HI). Since the logarithmic term varies much more slowly than N^2, it was argued that the experimental data for very long polymer chains will fit to $E_c\propto(1/N^2)(=1/M_w^2)$. However, computer experiments showed that for N as large as 500, the exponent (≈ 1.8) is significantly below the limiting value of 2. BDS using bead-spring chain has also been performed to probe chain breakage in transient elongational flow that mimics the deformation experienced by a chain as it translates along a streamline in an abrupt contraction device [Knudsen *et al.* (1995, 1996)]. In the presence of HI, the critical flow rate was found to be $\propto(1/N^p)$, $p=0.95\pm 0.2$ while if HI was neglected, $p=1.8\pm 0.2$. The closer agreement with experimental data ($0.95\leqslant p\leqslant 1.3$) obtained using HI suggested that in transient elongational flows, HI would retard the unraveling of the chains significantly more than that in steady flows. We note here that the flow in an abrupt contraction device is mixed, i.e., both shear and elongational deformations exist. Hence, it is plausible that prestretching of the chains by shear deformation could have a pronounced influence on the scission threshold. In fact, BDS using bead-spring chains performed by Hsieh *et al.* (2005) for a planar cross-slot flow precisely demonstrate this effect, i.e., the chains are prestretched by shear at the inlet section of the channel and break as they approach the stagnation point dominated by extensional deformation. Hsieh *et al.* (2005) defined chain scission to occur when any spring experiences a force over a preset critical spring force.

While the above approach based on bead-spring models and *ad hoc* energetic or instantaneous spring force criterion offers a computationally tractable route to predict the onset of chain scission, it also raises certain questions that hitherto have been unanswered. In the bead-spring models, the spring does not necessarily represent a chemical bond or an energetic link; rather it is of entropic origin. Hence, "scission" at the bead-spring *level* of description is at best ambiguously defined. As mentioned above, the criterion for scission in steady elongational flow ($E_c\propto\eta^{-1}M^{-2}$) can be anticipated based on the property of a Rouse chain to extend infinitely as $\lambda_H N^2 E\rightarrow\pi^2/4$. In other words, this criterion is a robust one independent of the specific form of the potential used. This is evident from BDS studies in the literature: Although the Rouse and Morse chains differ qualitatively in terms of the spring potential [see Fig. 1 in Lopez Cascales and Garcia de la Torre (1991)], they both yield practically identical results for the dependence of the scission threshold on the number of segments although the absolute value of the critical

strain rate is model dependent. For instance, for $N=20$, E_c for the Morse chain is approximately a factor of 3 greater than that for the Rouse chain. Hence, a protocol for the selection of model parameters in bead-spring simulations that would yield model-independent results is at best ambiguous. Data obtained from computer experiments performed using fine-grained models such as bead-rod chains could help parameter selection for coarser, bead-spring models. The selection of the scission criterion is also of great importance. In energy-based approaches, the scission parameters such as the bond dissociation energy cannot be estimated accurately. For the bead-rod chain, it is realistic to use a force-based criterion for chain scission since the "rod" represents the collection of monomers that move in a concerted fashion. Recent advances in atomic force microscopy (AFM) allow one to accurately determine the critical tension [Grandbois *et al.* (1999)]. However, a criterion based on instantaneous segmental tension (ST) suffers from certain numerical artifacts, since the time integration of stochastic differential equations describing the polymer chain dynamics leads to an increase in instantaneous ST fluctuations with decreasing time step dt as$(dt)^{-1/2}$. Motivated by these considerations, we have chosen to utilize BDS based on bead-rod chains in the present study and develop an algorithm to account for the effect of stochastic fluctuations in segmental tension on the scission probability so that dt-independent predictions can be obtained. While scission threshold is of vital interest, in practical applications, strain rates much greater than E_c are often used. Hence, it is also important to examine scission under the condition of $E \gg E_c$. It is plausible (as shown in this work) that partially uncoiled chains with sufficiently long contiguously extended portions could also break when $E \gg E_c$.

In general, one would expect the scission probability should not only depend on the instantaneous segmental tension but also on the "loading" rate, i.e., the rate at which the polymer is stretched. In other words, the probability of scission for a chain stretched very rapidly from equilibrium should be different from that for one unraveling at a very slow rate. In the context of flow-induced scission, such elongation rate dependence of scission probability has not been quantitatively studied. However, such effects have been studied in the context of the disentanglement from a substrate of a polymer chain pulled by a force exerted on the free end (e.g., using an atomic force microscope tip) [Evans and Ritchie (1997)]. As in the case of the thermally activated barrier to scission (TABS) models, [Bestul (1956); Zhurkov and Korsukov (1974)] the applied mechanical stress is expected to lower the activation energy barrier ΔE for scission, but the extent to which it is reduced depends on the pulling rate itself. This may be thought of as a generalization of the Bell model [Bell (1978)] originally proposed to study the effect of mechanical forces on cell adhesion on substrates. Evans and Ritchie (1997) argued that the probability of detachment of a polymer chain depends on both the reduction in the energy barrier to scission induced by the mechanical stimulus (applied force) and a hopping or attempt rate to overcome this barrier. The direct application of their theoretical results to flow-induced scission of free (i.e., nontethered) polymer chains is not straightforward. Note that for free chains ST vanishes at the chain ends, a scenario that is qualitatively different from the one in which tethered chains are pulled at their free ends. However, in general, one would expect the attempt rate and the reduction in the energy barrier to be functions of flow deformation rate since it has a direct influence in determining the loading rate e. As a result, following Evans and Ritchie (1997), one can express the probability of scission as a function of elongational rate $p(e)=g(e)\exp(-\Delta E(e)/kT)$ where $g(e)$ is the likelihood of dissociation contributed by tension fluctuations, and ΔE is thermal activation energy to overcome the transition state, which is lowered by the applied deformation rate e. In this work, we have analyzed and interpreted the scission probabilities predicted by the present algorithm within the framework of this extended TABS model.

This paper is organized as follows. In Sec. II, the governing equations and critical tension estimation for the Kramers (bead-rod) chain model are introduced along with a detailed discussion of the statistical properties of ST distribution and how they depend on model/simulation parameters such as chain length, flow strength and time-step size. This motivates the development of a new simulation algorithm for time-step size independent predictions of scission kinetics, presented in Sec. II C. Section III contains results and discussion for critical tension and kinetics of scission, probability density function (pdf) of cleaved (daughter) chains, the effect of hydrodynamic interactions and transient elongational flow on the scission threshold, and the effect of loading (extension) rate on scission probability. Conclusions are offered in Sec. IV.

II. SIMULATION METHODS

A. BDS of bead-rod chains

In a bead-rod chain, each bead represents a group of monomers of the polymer and the rod length is related to the persistence length, which is a measure of chain stiffness of polymer. BDS algorithms for Kramers chains have been presented in detail elsewhere [Doyle *et al.* (1997); Liu (1989)]. For a spatially homogenous velocity gradient and in the absence of HI, the stochastic differential equation governing the evolution of the position vector, $\mathbf{r}_i$, of bead i, $1 \leqslant i \leqslant N_k+1$, is given by

$$\frac{d\mathbf{r}_i}{dt} = \mathbf{v}_0 + [\boldsymbol{\kappa} \cdot \mathbf{r}_i] + \frac{1}{\zeta}(\mathbf{F}_i^C + \mathbf{F}_i^B), \tag{1}$$

where $\mathbf{v}_0$ is an ambient fluid velocity, $\boldsymbol{\kappa}$ is the transpose of the velocity gradient tensor, ζ is the hydrodynamic friction coefficient, $\mathbf{F}_i^C$ is the constraint force, and $\mathbf{F}_i^B$ is the randomly fluctuating Brownian force that represents the jostling of the polymer by the surrounding solvent molecules. Equation (1) is subjected to N_k constraints:

$$g_i = (\mathbf{r}_{i+1} - \mathbf{r}_i)^2 - a^2 = 0, \quad i = 1,2, \ldots, N_k, \tag{2}$$

where a is the rod length. The constraint force $\mathbf{F}_i^C$ acting on bead i can be evaluated as

$$\mathbf{F}_i^C = -\sum_k \gamma_k \frac{\partial g_k}{\partial \mathbf{r}_i}, \tag{3}$$

where γ_k $(1 \leqslant k \leqslant N_k)$ are Lagrange multipliers representing the STs. Neglecting its correlation with the constraint force, the Brownian force $\mathbf{F}_i^B$ can be shown to have the following statistical properties:

$$\langle \mathbf{F}_i^B(t) \rangle = 0, \quad \langle \mathbf{F}_i^B(t)\mathbf{F}_j^B(t') \rangle = 2k_B T\zeta\delta_{ij}\delta(t-t')\boldsymbol{\delta}, \tag{4}$$

where δ_{ij} denotes the Kronecker delta, $\delta(t-t')$ denotes the Dirac delta function, $\boldsymbol{\delta}$ is the unit tensor, and the angular brackets denote ensemble averaging.

In integrating Eq. (1), we follow Liu's approach [Liu (1989); Somasi *et al.* (2002)] where the bead position is updated by using a predictor-corrector algorithm. In the predictor step, the bead position $\mathbf{r}_i^*(t+dt)$ is updated without the constraint force:

$$\mathbf{r}_i^*(t+dt) = \mathbf{r}_i(t) + [\boldsymbol{\kappa} \cdot \mathbf{r}_i(t)] \cdot dt + \sqrt{\frac{2kT_B dt}{\zeta}}\Delta\mathbf{W}_i, \tag{5}$$

where $\Delta\mathbf{W}_i$ is the discrete random noise on bead i such that

$$\langle \Delta \mathbf{W}_i \rangle = \mathbf{0}, \quad \langle \Delta \mathbf{W}_i \Delta \mathbf{W}_j \rangle = \delta_{ij} \boldsymbol{\delta}. \tag{6}$$

In the corrector step, the predicted bead positions are corrected for the constraint force acting on the rod:

$$\mathbf{r}_i(t+dt) = \mathbf{r}_i^*(t+dt) - \frac{dt}{\zeta} \sum_k \gamma_k \frac{\partial}{\partial \mathbf{r}_i} g_k. \tag{7}$$

Coupling Eq. (2) with Eq. (7) results in N_k nonlinear equations for the STs, which can be solved iteratively until all constraints are satisfied within the specific tolerance.

During the time interval from t to $t+dt$, the fluctuating Brownian force acting on the bead i has the statistical properties [Gardiner (1985)]:

$$\langle \Delta \mathbf{F}_i^B(dt) \rangle = 0, \quad \langle \Delta \mathbf{F}_i^B(dt) \Delta \mathbf{F}_j^B(dt) \rangle = \frac{2k_B T \zeta \delta_{ij}}{dt} \boldsymbol{\delta}. \tag{8}$$

Equation (8) implies that the variance in the stochastic fluctuation $\propto (1/dt)$. Hence a chain scission criterion based on the instantaneous tension will *not* yield dt-independent results. This issue and how to circumvent it will be discussed later.

As discussed in Sec. I, HI has been shown to influence the critical strain rate predicted by BDS using bead-spring chains. For bead-rod chain, Öttinger (1994) has developed a BDS technique that allows accurate incorporation of HI. Although such simulations are computationally very expensive, we have performed a limited set of calculation to assess the role of HI on chain scission. In presence of HI the predictor step is modified as [see Eq. (25), Öttinger (1996)]:

$$\mathbf{r}_i^*(t+dt) = \mathbf{r}_i(t) + [\boldsymbol{\kappa} \cdot \mathbf{r}_i(t) + \sum_j \mathbf{H}_{ij} \cdot (\mathbf{F}_j + \mathbf{F}_j^{(m)})] \cdot dt + \sqrt{2kT_B dt} \sum_j \mathbf{B}_{ij} \cdot \Delta \mathbf{W}_j, \tag{9}$$

where $\mathbf{H}_{ij}$ is a tensor that determines the HI between bead i and j [see Eq. (10) below], $\mathbf{F}_j$ is the internal interaction force on bead j, $\mathbf{F}_j^{(m)}$ is an extra force due to the constraint [see Eq. (24), Öttinger (1994)], $\Delta \mathbf{W}_j$ is Gaussian random vectors with $\langle \Delta \mathbf{W}_j \rangle = 0$, and $\langle \Delta \mathbf{W}_i \Delta \mathbf{W}_j \rangle = \delta_{ij}\, \boldsymbol{\delta}$. $\mathbf{B}_{ij}$ is related to the HI tensor satisfy:

$$\mathbf{H}_{ij} \equiv \delta_{ij} \zeta_i^{-1} + \boldsymbol{\Omega}_{ij} = \sum_k \mathbf{B}_{ik} \cdot \mathbf{B}_{jk}^T, \tag{10}$$

where ζ_i^{-1} is a symmetric friction tensor, and $\boldsymbol{\Omega}_{ij}$ represents the Rotne–Prager–Yamakawa (RPY) tensor that is used in this study [Bird *et al.* (1987)]. The corrector step is expressed as [see Eq. (26), Öttinger (1994)]:

$$\mathbf{r}_i(t+dt) = \mathbf{r}_i^*(t+dt) - \sum_{k=1}^{N_k} \gamma_k \left[\sum_j \mathbf{H}_{ij} \cdot \frac{\partial g_k}{\partial \mathbf{r}_j} \right]_c. \tag{11}$$

The expression for the diagonal elements of RPY tensor is $H_{ii}^{\alpha\beta} = (kT/\zeta)\delta_{\alpha\beta}$ and the off-diagonal elements for nonoverlapping beads ($r_{ij} > 2a$) have the form:

$$H_{ij}^{\alpha\beta} = h^* \sqrt{\frac{\pi}{3}} \frac{3kT}{4\zeta} \frac{\sigma}{r_{ij}} \left[\left(\delta_{\alpha\beta} + \frac{r_{ij}^\alpha r_{ij}^\beta}{r_{ij}^2} \right) + \frac{2\sigma^2}{3r_{ij}^2} \left(\delta_{\alpha\beta} + \frac{3r_{ij}^\alpha r_{ij}^\beta}{r_{ij}^2} \right) \right], \tag{12a}$$

where r_{ij} is the distance between beads i and j, σ is the hydrodynamic radius, and $h^* = (3/\pi)^{1/2} \sigma/a$ is the parameter representing the strength of HI. If the beads are allowed to overlap ($r_{ij} < 2a$) this tensor is

$$H_{ij}^{\alpha\beta} = \frac{kT}{\zeta}\left[\left(1 - \frac{9r_{ij}}{32\sigma}\right)\delta_{\alpha\beta} + \frac{3}{32\sigma}\frac{r_{ij}^{\alpha}r_{ij}^{\beta}}{r_{ij}}\right]. \tag{12b}$$

Hereafter, we use the rod length, a, k_BT/a and $\zeta a^2/k_BT$ as characteristic scales for length, force and time, respectively. We define the Peclet number $\mathrm{Pe}=E(\zeta a^2/k_BT)$ as the ratio of bead diffusion time to characteristic flow time $1/E$ and the Weissenberg number $\mathrm{We}=E\lambda_{\max}$ where $\lambda_{\max}$ is the longest relaxation time of a bead-rod chain with N_k segments. For example, $\lambda_{\max}=0.0142\cdot N_k^2(\zeta a^2/k_BT)$ if HI effects are negligible [Doyle *et al.* (1997)]. If HI is incorporated, the exponent of N_k is 1.5–1.6 depending on the value of hydrodynamic interaction parameter h^* [Neelov *et al.* (2002)].

B. Critical tension estimation

In the simulations, it is required to determine whether the ST exceeds the bond rupture force, f_{rup}. Using the TABS model, Odell and Keller (1986) estimated f_{rup} for C-C bonds to be between 2.6 and 13.4 nN. Recently, the strength of a covalent bond has been measured by AFM [Grandbois *et al.* (1999)]. In these experiments, a single polymer chain that consists of hundreds of monomeric units is covalently anchored between a substrate and the tip of an AFM and stretched until bond scission occurs. It was observed, consistent with the theoretical predictions based on density functional theory (DFT), that the pdf associated with chain rupture is a Gaussian where the mean and variance depend on the atomic constituents. For instance, the rupture force (in nN) of Si–C bonds is found (experimentally) to be 2 ± 0.3 while the DFT prediction for the scission force for a Si–C bond is approximately 2.8. DFT predicts $f_{\mathrm{rup}}=3.7\sim4.3$ nN for a C–C bond. In this work, the dimensionless critical tension T_c for chain scission is estimated based on the average fracture force for C–C bond as

$$T_c \equiv f_{\mathrm{rup}}/[k_BT/a] \approx 10^5, \tag{12'}$$

where $a\approx100$ nm is chosen as the Kuhn step length of stained λ-phage DNA molecules studied by Larson *et al.* (1999). This translates to approximately 150 segments to adequately capture their configuration dynamics. Admittedly, the microstructure of biological and synthetic polymers in solution is often more complicated than that represented by a linear bead-rod chain. However, flow-induced configurational changes of such polymers can be captured semiquantitatively by BDS using bead-rod chains [Doyle *et al.* 1997; Doyle and Shaqfeh (1998); Perkins *et al.* 1997]. Since the ST distribution depends primarily on the chain configuration, BDS using bead-rod models should be able to provide sufficiently accurate results for the mean and variance in STs. Evidently, the choice of a is also system dependent. For instance, for flexible polymers such as polystyrene (PS) and poly-(ethylene oxide) (PEO), T_c becomes much smaller because of their relatively short Kuhn length. This implies that in order to represent a high M_w PS or PEO, thousands of segments would be necessary. This is computationally prohibitive. Hence in this work, we focus on relatively flexible macromolecules that have large Kuhn lengths and can be represented by O(10)-O(100) bead-rod segments. This allows us to study the effect of M_w on E_c. Moreover, as shown in Sec. III, scission kinetics should not be qualitatively influenced by the choice of T_c but rather on the ratio T_c/We.

C. Scission algorithm

In BDS, ensemble averaged properties can be shown to approach asymptotic values as dt becomes sufficiently small [Öttinger (1996)]. Utilizing the fact that the integration error decreases as $dt^{1/2}$ in the Euler method, extrapolation techniques have been devel-

oped to allow for the evaluation of the asymptotic values for rheological parameters from simulation data obtained using finite dt values. However, in order to determine whether a chain scission event has occurred, the *instantaneous* segmental tension (IST) has to be compared with the threshold value T_c discussed in the previous section. Since "convergence" with respect to dt for IST cannot be attained, any simulation that employs a comparison of its value with T_c (and decides that a chain scission event occurs when IST $>T_c$) will not be able to provide results for scission kinetics that are *independent* of dt. In the subsequent section, we demonstrate this and present a novel approach that can yield dt-independent result. The principal idea behind the development of the new technique is the experimental observation that *scission itself is a stochastic process* [Grandbois *et al.* (1999)] and via appropriate renormalization of the tension profile along the chain, it is possible to develop a universal profile that can be used to make a decision for chain scission.

1. Failure of instantaneous segmental tension (IST) criterion

In the literature, simulations of chain scission have been performed using instantaneous criteria; i.e., by comparing the instantaneous numerical value of a stochastic variable to a pre-determined critical one. For instance, a bead-spring chain was assumed to be cleaved if the stretching energy reaches some limiting value corresponding to a critical spring length [Knudsen *et al.* (1995, 1996); Lopez Cascales and Garcia de la Torre (1991, 1992); Reese and Zimm (1990)]. Although the above studies do not contain discussions of the influence of the dt size used in the simulation, it is perceivable that the use of an instantaneous scission criterion could present methodological difficulties. In order to illustrate this, we show in Fig. 1 the dt dependence of scission kinetics, as indicated by the plots of scission percentage, defined as $100(n\text{-}n_0)/n_0$ where n and n_0 denote the instantaneous and initial number of chains respectively, versus strain $\varepsilon \equiv Et$, and pdf of chain length predicted using the IST criterion, i.e., scission occurs when IST exceeds $T_c=10^5$. Figure 1(a) shows that for all cases, the number of chains increases with time and approaches asymptotic values. However, the total number of chains in the plateau region increases with decreasing dt. Moreover, scission is predicted to occur at earlier times as dt decreases. This means that, when the chain scission is determined based on IST, the simulations give different results depending on the *numerical* parameter dt even when identical initial configurations and physical parameters are used. The dependence of dt on scission kinetics also appears in the pdf of the daughter chains as shown in Figure 1(b). When the simulation time step is large ($m=6$), two peaks appear approximately symmetrically on either side of the midpoint ($N_k=50$) of the fully stretched chain. This means that scission occurred just one time at a distance of one third of the chain length from the chain end, which almost doubles the chain number and gives two most likely values of chain lengths, namely $N_k=35$ and 65. At the smallest time step used ($m=10$), the probabilities of chain length for less than $N_k=50$ increase, which implies that most of the chains greater than $N_k=50$ were cleaved more than once during the simulation.

In order to investigate the origin of the time-step dependence of scission kinetics, a large amount of simulation data for STs are collected and analyzed. Figure 2(a) shows the average and standard deviation in the tension along the fully stretched chain. The average tension $\langle T_k \rangle$ versus segment number k exhibits a parabolic shape and is well represented by the function

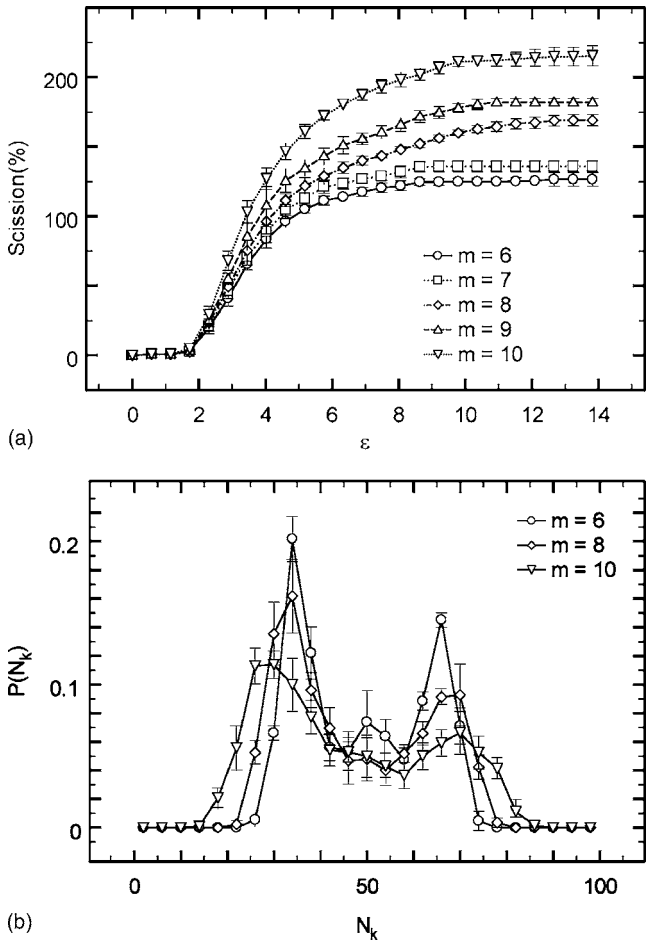

FIG. 1. Scission kinetics and pdf of chain length for $n_o=100$, Kramers chains ($N_0=150$) predicted by simulation that use the instantaneous ST criterion for different $dt=\Delta t/2^m$, $\Delta t=10^{-4}$ values. $We=20\,000$. $\varepsilon=Et$ (a) More scission events are predicted for small dt values. (b) The major peak in pdf is predicted to broaden and shift to the smaller molecular weight region with decreasing dt.

$$\langle T_k\rangle = T_o\left[1-\left(1-\frac{2k}{N_k}\right)^2\right], \tag{13}$$

where N_k is the number of segments in chain ($1\leqslant k\leqslant N_k$), and T_0 is the maximum average tension at the middle of a fully stretched chain. T_0 is a function of strain rate and chain length. Based on BD simulations for fully stretched Kramers chains in steady elongational flow, we find that T_0 can be expressed as

$$T_o = 0.125EN_k^2(\zeta a^2/k_BT). \tag{14}$$

Figure 2(a) also shows that the standard deviation in the tension is the largest at the middle of chain, and decreases toward the chain ends. Hence the most probable point of scission is the midpoint when the chain is fully stretched.

From the above simulation results obtained for different dt values, it is clear that the average tension is not affected by dt whereas the fluctuations are significantly influenced by it. It means that the ST fluctuations need to be taken into account in order to explain

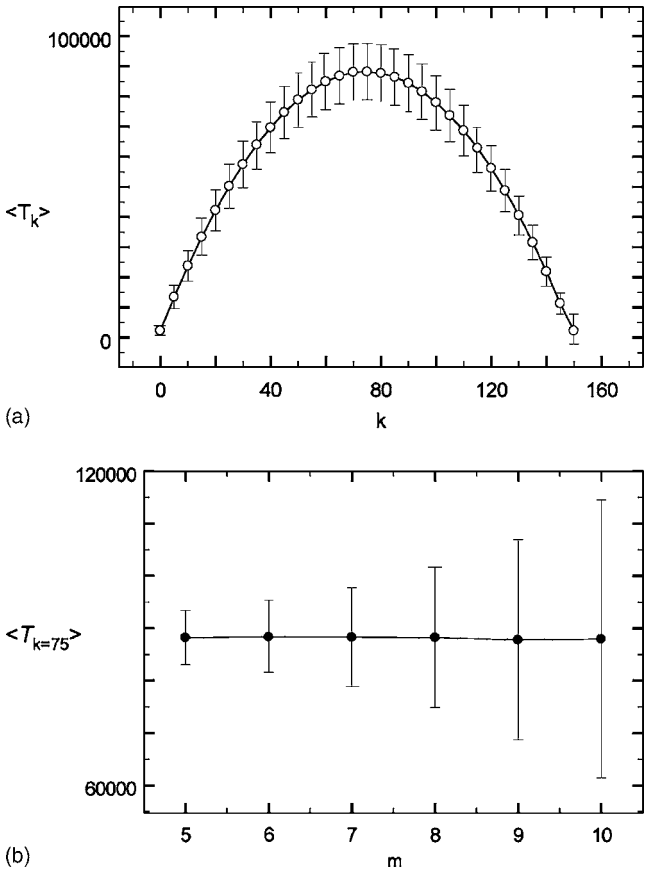

FIG. 2. Average and fluctuations of ST for fully stretched Kramers chain ($N_o=150$) at $We=10\,000$. (a) Average tension along the chain backbone has a parabolic shape ($m=7$). (b) ST fluctuations increase with decreasing dt, $dt=\Delta t/2^m$, $\Delta t=10^{-4}$.

the time-step effects seen in Fig. 1. Figure 2(b) shows the average and standard deviation of ST measured at the middle of chain, $N_k=75$, as a function of dt. As seen from Eq. (8), the statistical correlation of the Brownian force used in the numerical simulation is a function of dt. This is reflected in Fig. 2(b), which shows that the standard deviation in ST increases as dt decreases. Hence, the use of IST criterion can lead to the prediction of scission events even when $\langle T_k \rangle$ is less than T_c if the time step is sufficiently small. In the next subsection, we propose a suitable normalization to circumvent this problem.

2. Statistical properties of segmental tension

In order to develop an algorithm that predicts scission events independent of dt, it is instructive to analyze the ST distribution along the chain. Figure 3(a) shows the ST distribution at $k=15$ and $k=75$ for different dt values along a 150 segment chain. ST distribution becomes broader as dt decreases whereas average tension remains constant as shown in Fig. 2. Moreover, the fluctuations in ST depend on the relative segment position. However, the tension distribution can be normalized to a Gaussian distribution function, independent of k and dt, as shown in Fig. 3(b), by utilizing the transformation

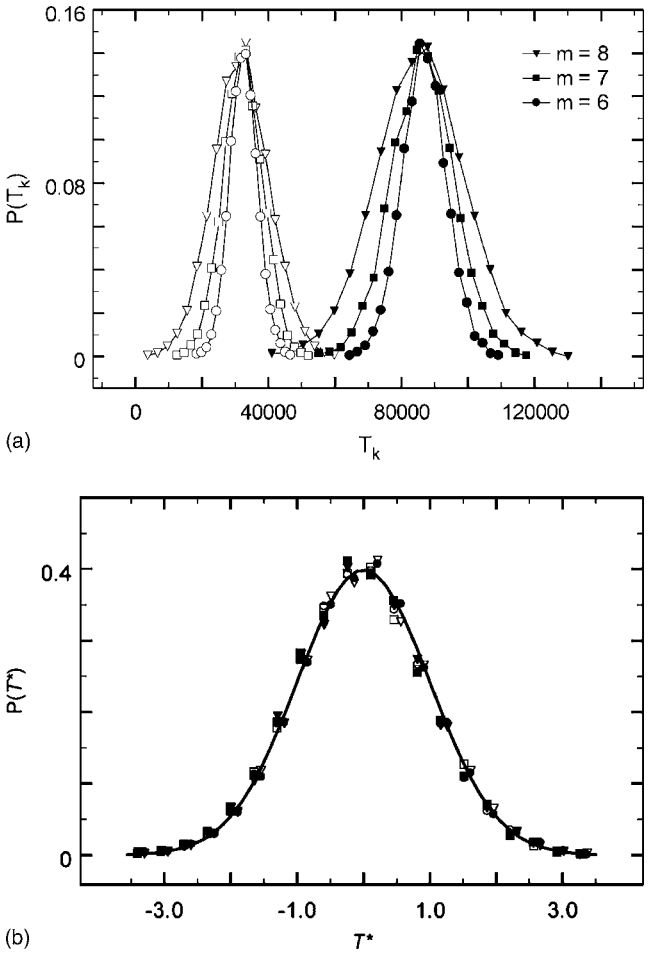

FIG. 3. The pdf of segment tension for a 150 segment chain at We=10 000. (a) pdf for $k=15$ (left) and $k=75$ (right) broaden with decreasing dt. (b) Figure 3(a) can be normalized by using Eq. (15) to obtain a Gaussian pdf (solid line) independent of the segment position k and time step dt.

$$T^* \equiv \frac{T_k - \langle T_k \rangle}{\sigma_k}, \tag{15}$$

where σ_k is the standard deviation of T_k, the tension in the kth segment. In Eq. (15), σ_k could be a function of elongation rate E, chain length N_k, and time-step dt; i.e., $\sigma_k = \sigma_k(E, N_k, dt)$. Figure 4 shows σ_k^2 versus k along a 150-segment chain for different dt values. The distribution of tension fluctuation has a parabolic shape and can be fitted by the expression

$$\sigma_k^2 = \sigma_o \cdot \left[1 - \left(1 - \frac{2k}{N_k} \right)^2 \right], \tag{16}$$

where the coefficient $\sigma_o = \sigma_o(k, E, N_k, dt)$.

In order to obtain an analytical expression for σ_o, a large number of simulations were performed with different values of dt and E for $N_k = 25, 50, 100$, and 150. As shown in Fig. 5, we found that if $\mathrm{We} = E\lambda_{max}$ is sufficiently large, the coefficient σ_o is only a

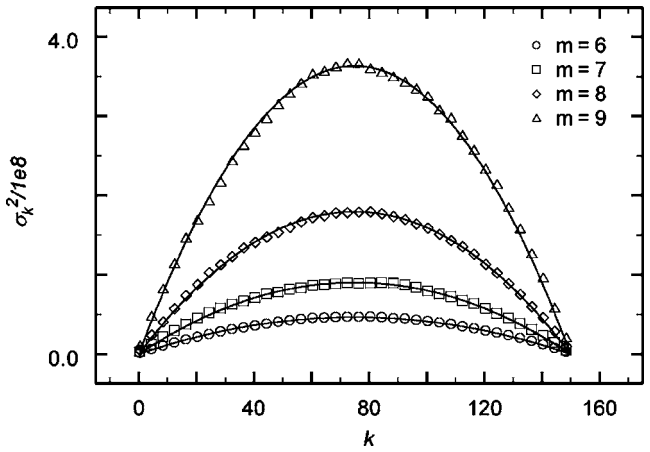

FIG. 4. Fluctuation in segment tension along the backbone of a 150 segment chain at $We = 10\,000$. Symbols are simulation data for different time step dt, and lines represent Eq. (16) with corresponding parameters for $dt = \Delta t/2^m$, $\Delta t = 10^{-4}$.

function of N_k and dt, i.e., $\sigma_o = \sigma_o(N_k, dt)$. This asymptotic independence of σ_o on We is illustrated in Fig. 5(b). From the simulations performed for $N_k = 10$, 25, 50, and 100 with $1 < \mathrm{We} < 100\,000$, we find that σ_o is independent of We for $\mathrm{We} > 1000$. In this asymptotic regime, it can be seen that [Fig. 5(b)]

$$\sigma_o = 0.527 \frac{N_k}{dt}. \tag{17}$$

Substitution of Eq. (17) into Eq. (16) gives an analytical expression for the standard deviation of tension in the kth rod within a fully stretched chain of N_k segments:

$$\sigma_k = \left\{ 0.527 \frac{N_k}{dt} \left[1 - \left(1 - \frac{2k}{N_k} \right)^2 \right] \right\}^{1/2}. \tag{18}$$

Equation (18), together with Eq. (14) for $\langle T_k \rangle$, can be used to find We, N_k and dt-independent, normalized segmental tension (NST) distribution T^* defined by Eq. (15).

3. Use of normalized segmental tension (NST) in scission algorithm

In experiments, the measured fracture force of a covalent bond was observed to have a broad distribution [Grandbois *et al.* (1999)]. Thus, it is reasonable for chain scission to be modeled as a stochastic event and incorporate the statistical properties of ST fluctuation presented in Sec. II C 2 into a new algorithm to predict scission events. Besides the statistical properties of fracture tension, the complexity in the conformational dynamics must be taken into account in the simulation. During the unraveling process, molecules undergo various conformational changes, the taxonomy of which can be expressed in terms of coiled, folded, kinked, dumbbell, and fully stretched conformations depending on the mass density of the chain along a characteristic direction, e.g., that of the end to end vector [Larson *et al.* (1999)]. Therefore, if the deformation rate is sufficiently high, the chain can be cleaved before it is fully stretched. In these cases, the coefficients of the average of and the fluctuations in ST in Eqs. (14) and (17) cannot be directly used in

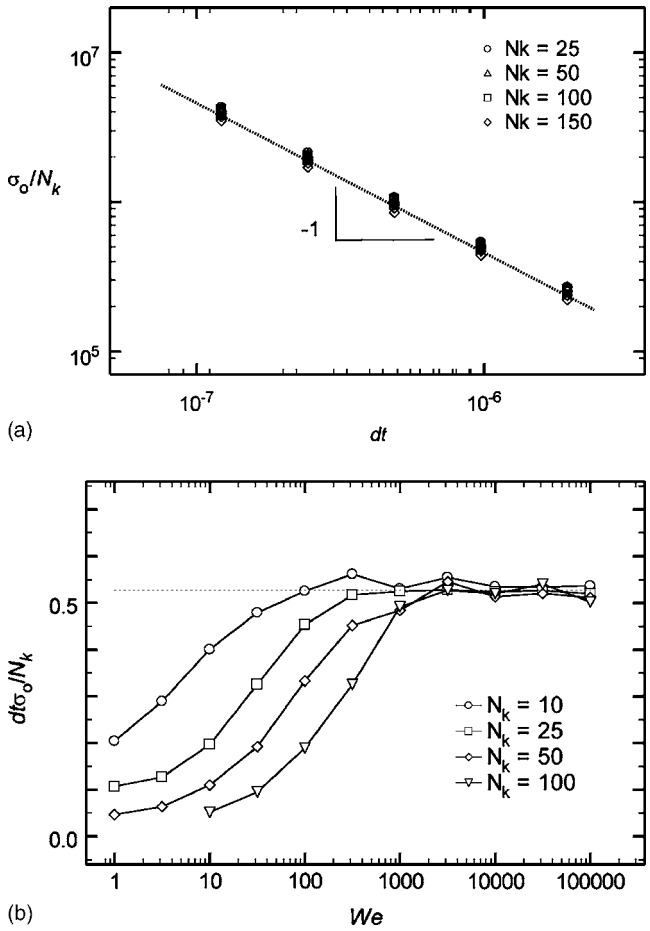

FIG. 5. (a) Log-log plot of the coefficient σ_o in Eq. (16) for different values of dt, N_k, and $8000 < \mathrm{We} < 16\,000$. (b) Log-log plot of σ_o for $1 < \mathrm{We} < 100\,000$.

chain scission simulation because they are obtained from a fully stretched configuration of N_k segments chain. As discussed below, we have developed an algorithm that can account for the configurational diversity.

Experimental observations [Grandbois *et al.* (1999)] suggest that the probability distribution of scission as a function of normalized tension T^* is Gaussian. Hence, the probability that a segment with tension T^* is fractured can be obtained by integrating the Gaussian distribution function

$$P_S(T^*) = \frac{1}{\sqrt{2\pi}} \int_{-\infty}^{T^*} e^{-z^2/2} dz. \tag{19}$$

Note that as expected from physical grounds, $P_S = 0$ as $T^* \to -\infty$ and approaches unity as $T^* \to \infty$, as implied by Eq. (19). While probing for a scission event, we locate the instantaneous maximum tension $T_{\max}$ within a chain of N_k segments. Subsequently, we identify the contiguously stretched chain portion within which $T_{\max}$ occurs as well as the number of the partially stretched segments N_p contained in this stretched portion of the chain. Note that $N_p \leqslant N_k$, with the equality implying a fully stretched chain. Moreover, N_p is

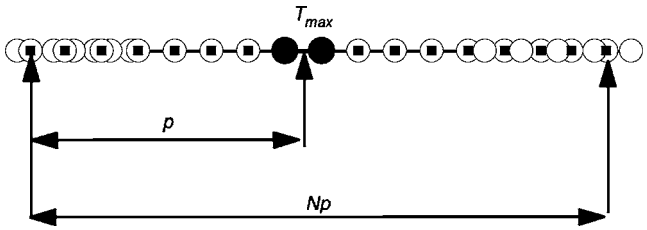

FIG. 6. Schematic of a partially coiled chain. The circles with square dot represent the contiguous extended portion of N_p segment in which the maximum instantaneous tension $T_{\max}$ is located. The position p for $T_{\max}$ is counted from the end of the stretched chain portion.

typically $\gg 1$. The segments within the stretched portion are numbered as shown in Fig. 6 from $p=1,2,\ldots,N_p$. We then normalize the instantaneous maximum tension by applying the transformation

$$\tilde{T}^* = \frac{T_{\max} - \langle T_p \rangle}{\sigma_p} + \frac{\langle T_p \rangle - T_c}{\sigma_G}, \tag{20}$$

where $\langle T_p \rangle$ is the average of and σ_p is the standard deviation in the tension at the pth segment along the partially stretched, N_p-segment chain portion. The variables $\langle T_p \rangle$ and σ_p are calculated from Eqs. (13) and (18) after replacing N_k with N_p. σ_G represents the standard deviation in the bond rupture force. The molecular parameters, σ_G and T_c, are obtained from single chain rupture experiments or flow-induced scission experiments. The first term on the left-hand side is the normalization of the instantaneous tension and the second is a shift factor scaled with respect to the standard deviation σ_G in the bond rupture force. We now compare the scission probability $P_S(\tilde{T}^*)$ with a uniformly distributed random number x, $0 \leqslant x \leqslant 1$. If $P_S(\tilde{T}^*) > x$, the segment is predicted to be cleaved. After fragmentation, the total number of Kuhn steps is kept constant by adding a bead on either of fractured chain ends by random selection. We note that the normalization procedure described above was obtained from an analysis of tension distribution in a fully stretched chain. The implicit assumption in the new algorithm is that the normalization procedure would apply to the extended portion of the chain even when it is a partially coiled state (Fig. 6). Since the characteristic time scales of the deformation rate and that associated with the delocalization of molecular vibrational energies are well separated, it appears that the statistical properties of the segment tension for the transient partially coiled configuration are not much different from those of the steady state configuration [Odell and Keller (1986)].

4. Use of instantaneous deterministic segmental tension

For bead-rod chains, it is possible that scission criterion can be replaced by an instantaneous, deterministic tension (IDST) derived by Schieber and Obasanjo (2005). The authors divided the constraint tension into an instantaneous, deterministic segmental tension (IDT) and a stochastic part. They derived an expression for IDST as a function of the deformation rate and chain configuration given by

$$\gamma_k = \zeta a \sum_i \hat{A}^{-1}_{ki} \boldsymbol{\kappa}:\mathbf{u}_i\mathbf{u}_i + \frac{6kT}{a}\sum_i \hat{A}^{-1}_{ki} - \frac{kT}{a}\sum_{i,m,n} A_{im}A_{in}\hat{A}^{-1}_{ik}\hat{A}^{-1}_{mn}(\mathbf{u}_m \cdot \mathbf{u}_n), \tag{21}$$

where u_i is the unit vector pointing from bead i to bead $i+1$, $A_{ij} := \Sigma_\nu \bar{B}_{\nu i}\bar{B}_{\nu j}$ is the Rouse matrix, $\hat{A}_{ij} := \Sigma_\nu (\mathbf{u}_i \cdot \mathbf{u}_j)\bar{B}_{\nu i}\bar{B}_{\nu j}$ is the Kramers matrix where $\bar{B}_{vj} = \delta_{v+1,j} - \delta_{v,j}$. The scission algorithm is simplified if this criterion is used, i.e., a scission event occurs when the IDST $> T_c$. We will present a comparison between the predictions obtained using the normalized tension (NST) and IDST criterion in the subsequent section.

5. Statistics of ST in presence of HI

The incorporation of HI into the chain dynamics changes the tension profiles along the chain in addition to the delay in unraveling of coiled chain. Hydrodynamic shielding induced by neighboring beads decreases the segment tension [Agarwal and Mashelkar (1994); Lopez Cascales and Garcia de la Torre (1991)]. Expressions analogous to Eq. (21) are not available in the presence of HI. Hence, we have performed statistical analysis similar to that described above for bead-rod chains in presence of HI leading to the development of equations analogous to Eqs. (13) and (18) to help probe for scission events. Specifically, we used $h^* = 0.244$ and found that the expression for the coefficients of the average of and the fluctuation in tension become $T_o = 0.1555EN_k^{1.7}$ and $\sigma_o = 0.7255N_k^{0.78}/dt$, respectively. The scission algorithm described in Sec. II C 3 is modified accordingly for cases with HI.

III. DISCUSSION OF RESULTS

A. Time-step independence of scission kinetics

As discussed above, we choose $T_c = 10^5$ and, $\sigma_G = T_c/50 = 2000$, which is motivated by experiments [Grandbois *et al.* (1999)]. During the simulations we probe for scission events at every $\Delta t = 10^{-4}(\zeta a^2/k_BT)$, which is much smaller than λ_{max} or $1/E$. Figure 7 shows the simulation results for scission kinetics obtained with different dt values at We = 24 000. The parameters used in this simulation are the same as the ones reported in Fig. 1. With the new algorithm, however, the nonphysical dt dependence of scission kinetics is eliminated so that the number of total chains n approaches a dt-independent, statistically converged value n_∞ as the strain becomes $\gg 1$ [Fig. 7(a)]. The ratio $n_\infty/n(t=0)$ lies between 2.16 and 2.21, and no systematic correlation is observed between the stochastic variability in n_∞ and dt. The pdf of daughter chain lengths, $P(N_k)$, for long times, shown in Fig. 7(b), is also independent of dt. The pdfs obtained for different dt values have two peaks at $N_k = 35$ and 65 implying that many chains break far from the middle. This shows that MSH does not hold for very strong flows that generate chain tension values that well exceed the threshold value T_c. This is consistent with the BDS predictions obtained using bead-spring models [Lopez Cascales and Garcia de la Torre (1992); Reese and Zimm (1990)]. We discuss the effect of flow strength in detail in the next subsection.

B. Effect of scission criterion: NST versus IDST

Figure 8(a) compares scission kinetics obtained by using the NST and IDST criterion for $We = 12\,000$, 24 000, and 48 000 while Fig. 8(b) shows the chain length pdf after scission for $We = 24\,000$. At $We = 12\,000$, which is marginally above $We_c = 11\,000$, there is little difference in the scission kinetics obtained using the two criteria. Moreover, it was found that for this value of We, pdf of daughter chain lengths is consistent with MSH as

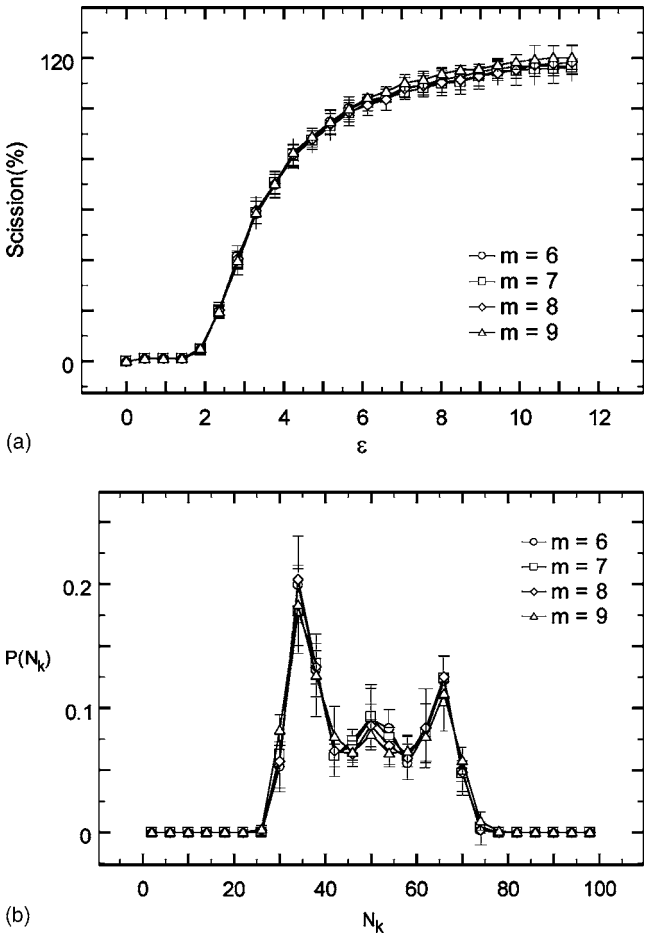

FIG. 7. Simulation results for steady elongational flow obtained by using the NST algorithm for a 100 segment chain at $We=24\,000$ for different $dt=\Delta t/2^m$, $\Delta t=10^{-4}$ values. Each simulation uses the same initial configuration ($n_o=100$). (a) The number of chains predicted is statistically independent of the dt value used in the simulation. (b) The predicted pdf of chain length is also dt independent.

shown in Fig. 9(a). However, the use of IDST criterion results in relatively narrow chain length distribution as compared with that obtained using NST criterion, which, due to the presence of ST fluctuations, predicts a broader distribution centered at the midpoint of the mother chains. At $We=24000$, $n_\infty/n(t=0)=2$, and 2.21 for IDST and NST criterion, respectively. Since the simulations use the same initial configurations and dt, the differences originate from the stochastic nature of the normalized tension criterion. Figure 8(b) shows pdfs of chain length for long times for $We=24\,000$. The major difference is the occurrence of more pronounced maxima predicted by the IDST criterion. Stochastic ST fluctuations can result in the breakage of partially coiled or folded chains if the extended portions are large enough to generate *average* tension values in the neighborhood of (but not necessarily greater than) T_c. Such fluctuations (which increase as We is increased) are incorporated into the NST criterion. Hence, it predicts more scission events and more frequent scission near the chain ends for We values that well exceed We_c. It was found for $We=24\,000$ and $48\,000$ scission occurred in some daughter chains as well. For instance, the longer of the two daughter chains resulting from a first scission at $N_k\approx 70$ can be fully

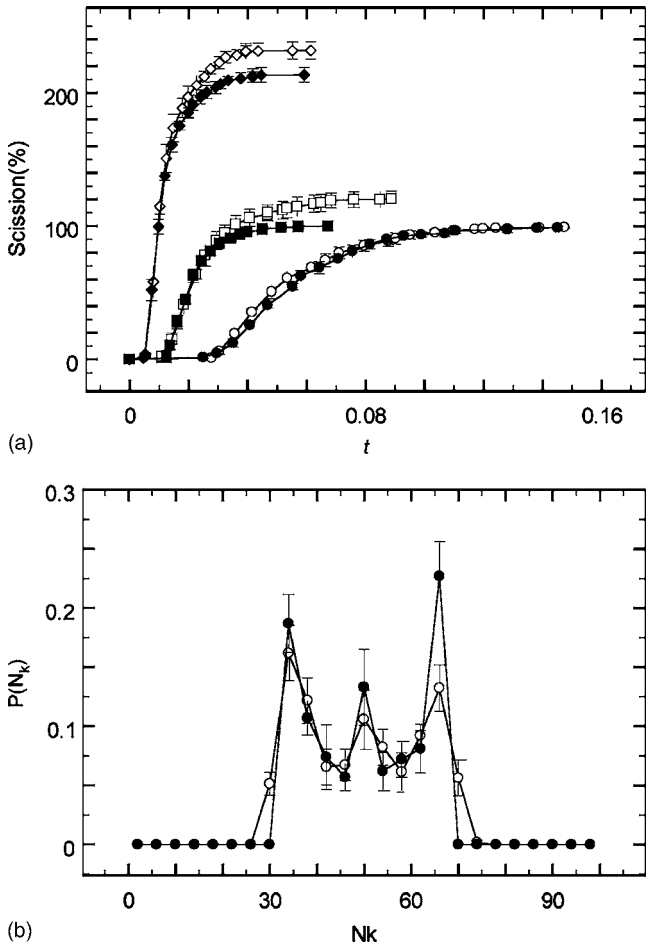

FIG. 8. (a) Scission kinetics obtained based on different criteria at $We=12\,000$ (circles), 24 000 (squares), and 48 000 (diamonds). Filled symbols are for IDST and open symbols are for NST criterion. (b) pdf for chain length distribution at $We=24\,000$. Filled symbols are for IDST and open symbols are for NST criterion.

stretched and broken again in the middle giving rise to two chains with 35 segments each. The probability of secondary scission is much larger with the NST criterion (due to the presence of ST fluctuations) and this is reflected in the more pronounced peak in the pdf [Fig. 8(b)] at $N_k \approx 35$.

C. Midpoint scission hypothesis

In steady elongational flow for $T^* \approx T_c$, chain scission is typically assumed to occur at the middle of the chain when the fully stretched configuration is achieved. The critical elongational rate, E_c, for MSH was observed to be inversely proportional to the square of the molecular weight or equivalently, for Kramers chains with N_0 segments, $E_c \propto 1/N_0^2$ [Odell *et al.* (1988); Horn and Merrill (1984)]. From the simulations performed for $N_o = 25$, 50, 100, and 150, we found that $10\,000 < We_c < 11\,000$ regardless of the chain length. This is consistent with the inverse square law dependence of E_c on N_o since $\mathrm{We} \equiv \lambda_{max} E \propto N^2 E$ for Kramers chains. The chain length pdf for $\mathrm{We}=12\,000$ is shown in Fig. 9(a). It is evident that the chains are primarily cleaved at the middle regardless of the

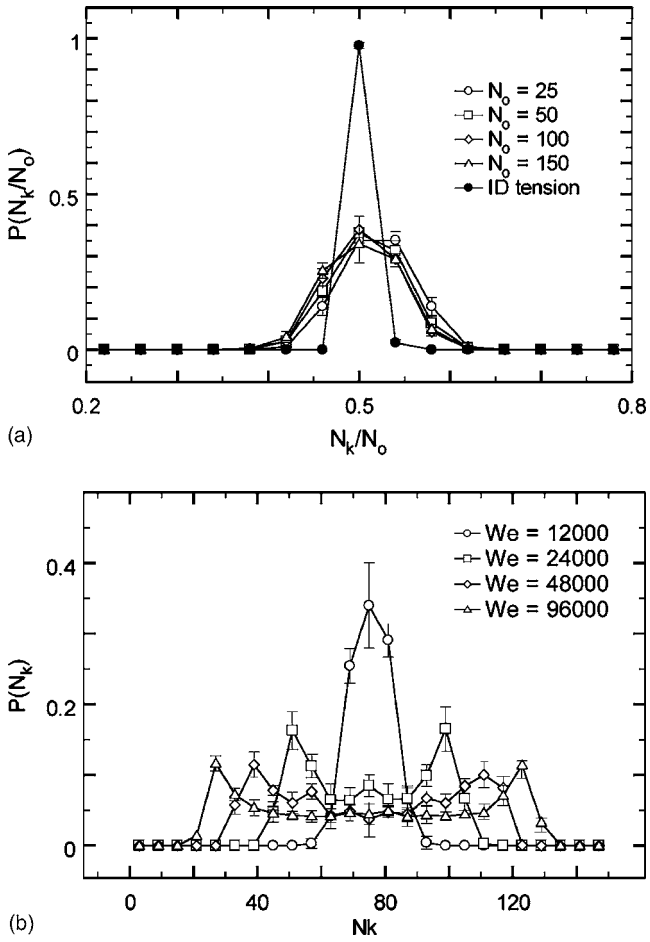

FIG. 9. (a) The *pdf* of molecular weight distribution normalized by the mother chain length at $We = 12\,000$. Chain scission occurs most likely at the middle of the chain regardless of the chain length. (b) At high *We*, the number of midpoint scission events decreases and more chains break in a partially coiled state.

mother chain length when the elongation rate is just above the threshold value. This implies that, even though the initial configuration influences the unraveling path of a chain in elongational flow [Larson *et al.* (1999)], the "individualism" in the single chain dynamics does not affect the pdf of chain length at $\mathrm{We} \approx \mathrm{We}_c$. When $\mathrm{We} \approx \mathrm{We}_c$, the chain needs to be stretched fully to allow for $T_{\max} \approx T_c$. However, as discussed above, if a coiled chain is abruptly subjected to a very strong flow, MSH is not strictly applicable even in steady elongational flow. Specifically, the larger the value of E (We), the greater the departure from the midpoint scission scenario. This is illustrated in Fig. 9(b), which shows that as We is increased, the chain length pdf becomes progressively broader (the mother chains are allowed to break only once in these simulations). For $\mathrm{We}/\mathrm{We}_c > 2$, the peaks appear in the pdf on either side of the midpoint and these peaks move farther away from the center as We is increased.

D. Configurational diversity

While most chains break in the fully stretched state near We_c there are diverse chain configurations at the moment of scission for $\mathrm{We} > \mathrm{We}_c$. Figure 10 shows different con-

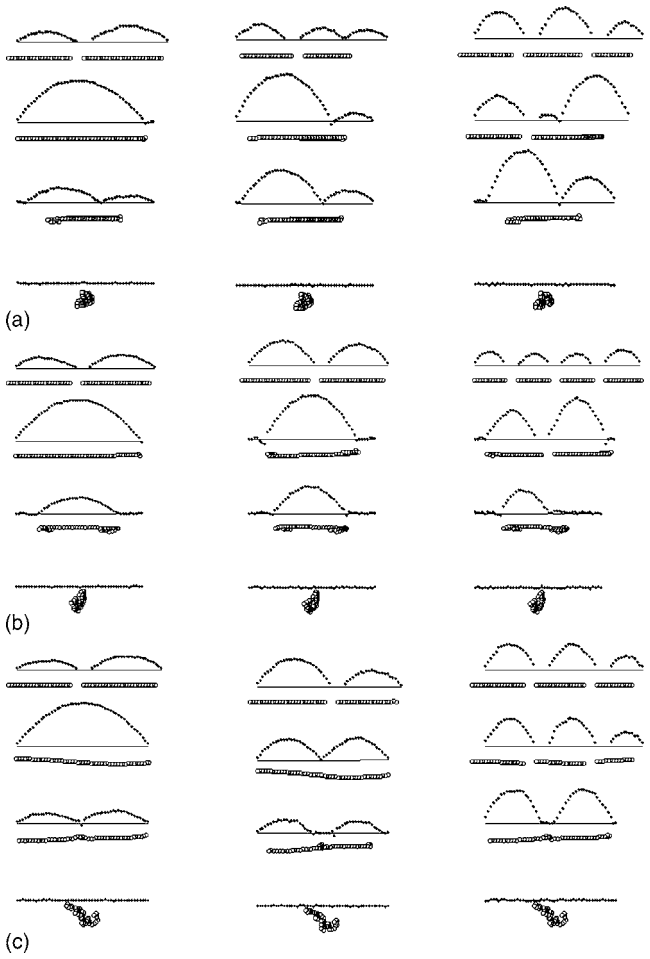

FIG. 10. Transient configurations and instantaneous tension along the chain backbone at the moment of scission for $We = 14\,000$, 28 000, and 56 000 (for each column from the left). (a) Folded, (b) Dumbbell, and (c) Kinked configurations.

figurations at the moment of scission and the corresponding instantaneous tension profile starting from different initial configurations. The chains could achieve folded, dumbbell, or kinked (knotted) configurations before scission occurs as shown in Figs. 10(a)–10(c), respectively. At $We = 14\,000$ [first column in Figs. 10(a)–10(c)], however, MSH holds regardless of the unraveling path. At $We = 28\,000$, the folded configuration, Fig. 10(a), can be cleaved far from the midpoint as its unfolded segment length can allow for tension to reach T_c before it is fully stretched, which can give the peaks in the pdf of chain length shown in Fig. 7(b). For the dumbbell configuration, if it has symmetric coiled ends during unfolding process as shown in Fig. 10(b), the scission occurs at midpoint during the process of unraveling. Similarly, Fig. 10(c) shows that if the chain is in the kinked configuration, far from midpoint scission is possible if the "knot" is near the chain ends such that the unknotted portion of chain develops instantaneous ST within the neighborhood of T_c.

At We=56 000 [third column of Figs. 10(a)–10(c)] the effect of configurational diversity on chain scission is significantly more pronounced. In the folded configuration, the

first scission occurs at nearly one third of the mother chain length and the second happens around the middle of the longer daughter chain after it is unfolded leading to a total of three chains in the final state. In the symmetric dumbbell configuration, scissions could occur twice at the middle of the original and daughter chains: First in the dumbbell state, and then after the daughter chains unravel almost entirely leading to a total of four chains in the final state. For the kinked configuration, scission occurs simultaneously at segments located one and two thirds of chain length along the chain backbone if the knot is placed in the middle. If the knot is far from the middle, the second scission can be delayed until the daughter chain with the knotted segments unravels to gain a sufficient tension.

E. Effect of critical tension, elongation rate, and chain length

As mentioned in Sec. II B, the critical tension is scaled by a force unit, k_BT/a where a is the Kuhn step length in the Kramers chain model. The Kuhn step length represents the "flexibility" of polymer, which is a molecular property that depends on the details of the chemical structure and solvent-polymer interactions. Hence, T_c values would also be system dependent. Motivated by this, we have performed a set of simulations to assess the effect of T_c on scission kinetics and the findings are summarized below.

Figure 11(a) shows the percentage increase in chains due to scission as a function of the elongational strain $\varepsilon=Et$ for $N_o=150$ for different values of We and T_c. As We is increased, scission occurs at smaller values of ε and the kinetics become progressively more rapid. However, note that the data sets that correspond to the same We/T_c ratio overlap with one another regardless of their critical fracture tension T_c. Similarly, the final chain length pdfs of daughter chains for cases that correspond to the same We/T_c are also statistically indistinguishable [see Fig. 11(b)]. We further note that this conclusion is valid for the chain length pdfs in the transient region as well.

Simulations were also performed with different mother chain lengths, N_o, at E values above the critical one to investigate the effects of chain length on scission. Figure 12 shows the simulation results for the scission kinetics and pdf of molecular weight. Figure 12(a) shows that shorter chains break faster since they unravel more rapidly [Doyle and Shaqfeh (1998)]. As the strain becomes $\gg 1$ an asymptotic state is achieved. The total number of chains at this state gradually increases with the length of the mother chain: $n_\infty/n(t=0)=2.12$, 2.19, 2.2, and 2.25 for $N_o=25$, 50, 100, and 150, respectively. This slight increase in $n_\infty/n(t=0)$ with increasing N_o is due to the increased ST fluctuation for longer chains [see Eq. (17)]. The final chain length pdfs are shown in Fig. 12(b). For shorter chains ($N_o=25$), the location of the first peak shifts to right as compared with those of longer chains, which can be attributed to the reduction in ST fluctuations with chain length.

F. Effect of HI and polymer residence time on critical strain rate

In order to ascertain the effect of HI on the longest relaxation time, we performed a number of simulations by varying N_0. In these simulations, fully extended chains were allowed to relax to their equilibrium configurations and their end-to-end distances were tracked as function of time. By fitting the latter stages of the dynamical data to an exponential function, the longest relaxation time $\lambda_{\max}$ can be obtained [Somasi *et al.* (2002)]. Figure 13(a) shows the effect of HI on $\lambda_{\max}$ for different chain lengths. The N_0 exponent for Kramers chains is found to be ≈ 2 while with HI, the exponent decreases to 1.54. These results are consistent with the predictions of Neelov *et al.* (2002) who examined the effect of HI on the extension rate E_{cs} at the onset of coil-to-stretch transition.

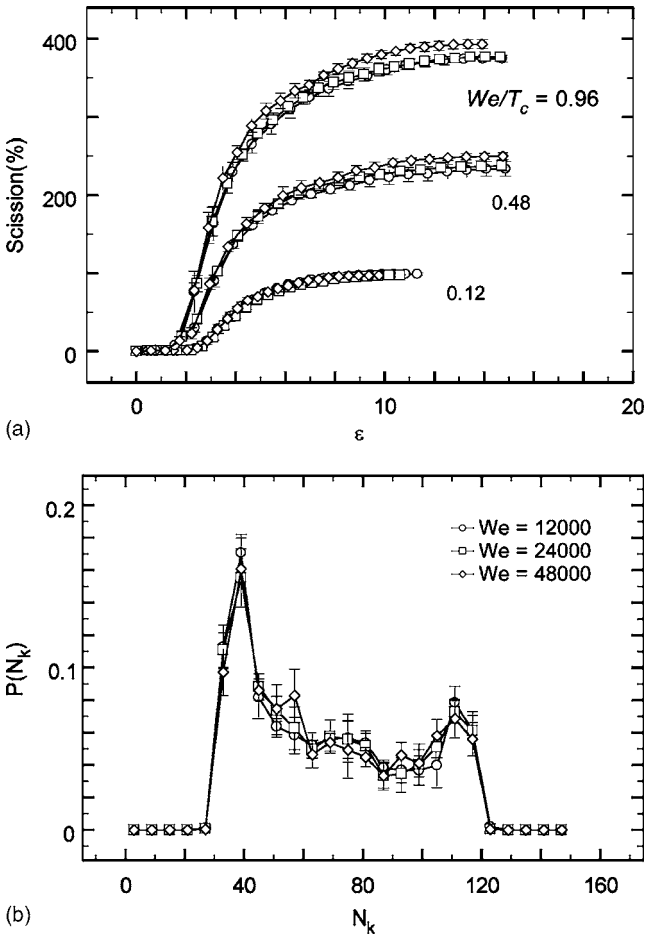

FIG. 11. Superposition of simulation results from different *We* and critical tension T_c for a 150-segment chain. (a) Scission kinetics at $\mathrm{We}/10^3=\{(3,6,12),(12,24,48),(24,48,96)\}$ with $T_c/10^3=(25,50,100)$ from bottom to top, respectively. Each group of three curves has the same We/T_c ratio as indicated. (b) The pdf's of chain length obtained for different *We* for $\mathrm{We}/T_c = 0.48$.

They found that E_{cs} is proportional to N_0^{-2} for Kramers chains while in presence of HI the N_0 exponent increased to ≈ -1.55. Since coil-to-stretch transition is known to occur when $\lambda_{max}E_{cs}\approx\frac{1}{2}$, these results imply that $\lambda_{max}\propto N_0^2$ and $N_0^{1.55}$ for cases without and with HI, respectively. This is consistent with results of the present study.

We further examined the effect of HI on the critical elongation rate for the onset of chain scission. Figure 13(b) shows the simulation results for the scission kinetics for different values of N_0. The critical elongation rate is found to decrease with N_0 as $E_c \propto N_0^{-1.7}$. As described in Sec. II C 5, in presence of HI, the average ST $T_0\propto N_0^{1.7}$. This is consistent with the N_0 dependence of E_c since near the critical elongation rate, the chains are cleaved mostly in the fully stretched configuration $T_c\approx T_o=0.1555\dot{\varepsilon}N_0^{1.7}$. Simulations based on energetic scission criterion and bead-spring models yield the N_0 exponent of $\approx$1.65 and 1.6 for the Rouse and Morse chains, respectively [Lopez Cascales and Garcia de la Torre (1991)]. An increase in the number of degrees of freedom in the chain is expected to increase the exponent: Asymptotic behavior for strong flows is given by $E_c \propto N_0^{-2}/\ln(N_0)$ such that for very large N_0, the experimentally observed behavior E_c

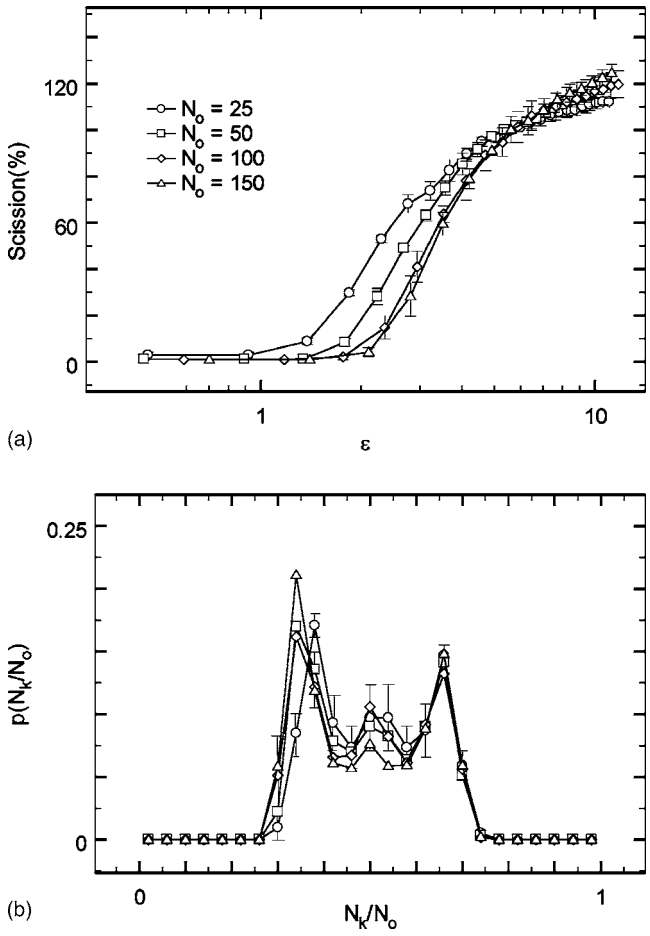

FIG. 12. Scission kinetics and pdf for molecular weight from different mother chain length at $We=24\,000$ and $T_c=10^5$. (a) Beginning of chain scission for short chain occurs earlier than that of long chains whereas the final results for percentage scission are nearly independent of chain length. (b) The pdf of 25-segment chain shows narrower distribution as compared with those for longer chains.

$\propto N_0^{-2}$would be recovered [Lopez Cascales and Garcia de la Torre (1991)]. However, as mentioned in the Sec. I, computer experiments using bead-spring models showed that for N as large as 500, the exponent (≈ 1.8) is significantly below the limiting value of 2. One plausible explanation is that excluded volume effects, not considered here, could increase the rate of chain unraveling resulting in breakage at lower values E. At this point, computational cost prohibits simulations with HI for $N_0 > 100$.

As mentioned in the Sec. I, in fast transient flows (FTF) such as the one created in an abrupt contraction device [Nguyen and Kausch (1988); Rabin (1988)], $E_c \propto 1/N_0$. The weak dependence of scaling law in FTF was explained by the combined effect of hydrodynamic interactions on chain unraveling [Nguyen and Kausch (1988); Rabin (1987)] and the shorter residence times that the polymer spends in the flow field. We have explored the effect of the latter on scission kinetics (in the absence of HI) by performing scission simulations for polymers that traverse the centerline of an abrupt contraction device. The flow field and geometry for the contraction flow are identical to those used by Knudsen *et al.* (1996) in the context of bead-spring chain simulations. It is a simplified

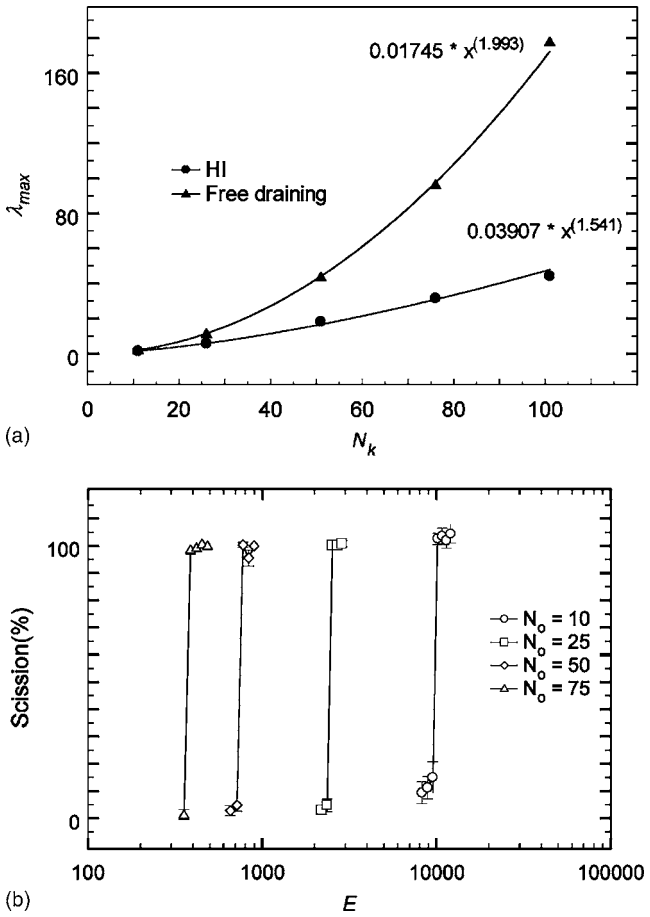

FIG. 13. (a) Longest relaxation time vs. number of segments for bead-rod chains with and without H.I. (b) Scission kinetics vs E for different chain lengths with HI effects

flow model that represents the transient elongational deformation in an axisymmetric contraction flow where the inlet and outlet radius of 1.0 and 0.02 cm, respectively (Fig. 14). The elongation rate in the converging flow region is modeled by that created by a mass flow sink as $E=4Q/\pi r^3$ where Q is the flow rate and r denotes the distance from the contraction plane. In order to avoid the singularity in E at $r=0$, the maximum extension rate is selected as the value of E at $r=0.02$ cm (outlet radius).

In the contraction flow described above, the chain experiences an extensional flow field only for a very short time compared with its longest relaxation time so that the chain can traverse the orifice before it is fully stretched. Because of short residence time, only a small fraction of chains could be cleaved in contraction flow even though the flow rate is greater than the threshold value [Nguyen and Kausch (1988)]. In the simulations, we place chains at different distances from the orifice and compute their trajectories as they translate along the centerline. The distance from the sink orifice is chosen such that for each chain length the ratio R of the residence time to the longest relaxation time is maintained constant. From simulations performed for R ranging between 0.001 and 0.2, we found that the critical volumetric flow rate Q_c for the scission approaches an asymptotic value for $R>0.05$. Figure 15 shows simulation results for the scission yield

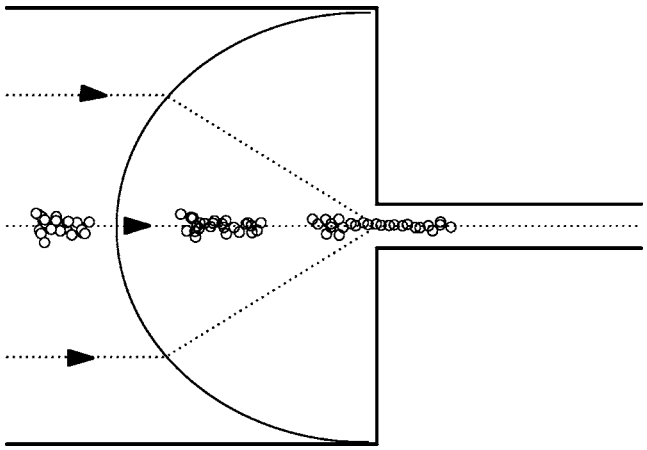

FIG. 14. Schematic of the transient elongational deformation in contraction flow.

with increasing Q for different N_0 and R values. From the critical volumetric flow rate $Q_c = \pi r^3 E_c/4|_{r=0.02}$ we found that $E_c \propto N_0^{-7/4}$ for $R > 0.05$. The weaker dependence of critical elongation rate on the chain length as compared with that for steady elongational flow is accounted for by the short residence time that necessitates larger elongational rates to cause the scission. The effect of HI can further slow down the unraveling process, leading to further increase in the critical tension. Simulations that incorporate HI into transient elongational flow are required to investigate this; such simulations using bead-rod chains are computationally expensive and hence are not reported here. If one assumes the effect of HI (on the N_0 exponent) in transient flows is similar to that in steady elongational flow (in which introduction of HI changes the exponent from 2 to 1.7), this would result in the prediction $E_c \propto N_0^{-p}$ where $p \approx 3/2$. This is still significantly different from unity observed experimentally for scission threshold in contraction flow devices, which suggests that preshearing could play an important role in configuration dynamics

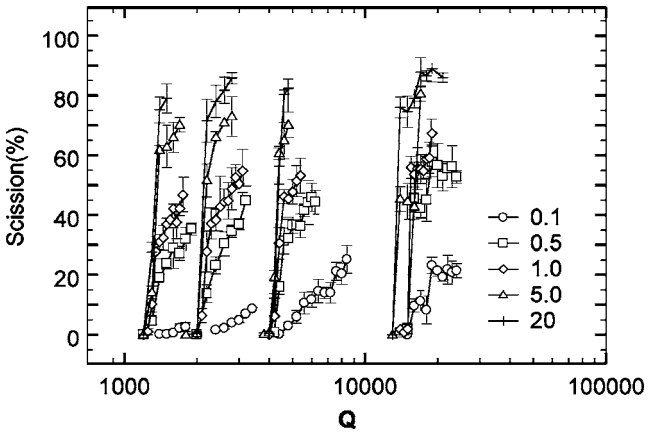

FIG. 15. Simulation results for the contraction flow for different residence times (measured as fraction of the longest relaxation time; see legend) and N_0.

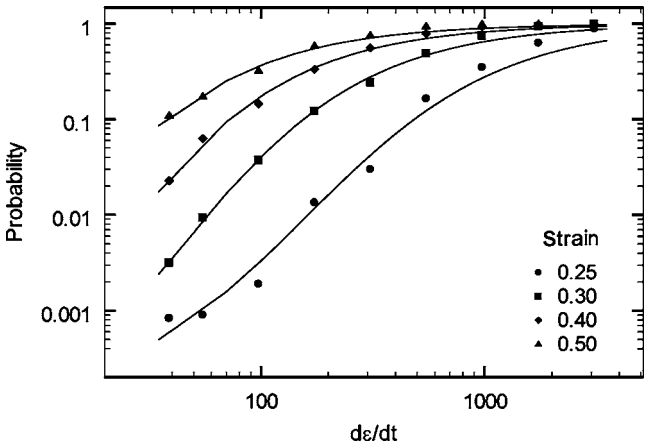

FIG. 16. Probability of scission as function of elongation rate for different strain values.

and scission in such flows. Moreover, it is also possible that if the shear rates are sufficiently large, the chains may break since they could unravel fully from a coiled state before tumbling events occur.

G. Dependence of scission probability on loading rate

As discussed in Sec. I, extended TABS-based theories suggest that the scission probability should depend on the rate at which the chain is stretched from a coiled to extended state such that $p(e)=g(e)\exp(-\Delta E/kT)$ where ΔE is the activation energy barrier to scission and e is interpreted as a time rate of increase in molecular extension rather than the applied elongational deformation. For free chains in flow the unraveling rate depends on the applied deformation rate E. Hence, we choose the elongation rate as the parameter that qualitatively represents the loading rate and examine the dependence of the scission probability predicted by the algorithm on the loading rate at constant strain values. The results are reported in Fig. 16. It can be seen that p increases with increasing elongation rate before saturating to unity for sufficiently large values of E. Although in the simulations the critical tension distribution for bond scission is not a function of the loading rate (E), the number of macromolecular scission events is significantly affected by the imposed extension rate. Specifically, as the extension rate is increased, the probability of finding straight sections [at length scales significantly above the persistence length; see Figs. 10(a)–10(c)] that possess segmental tension in the neighborhood of its critical value increases. Hence, the enhanced scission at high loading rates is a consequence of the modification of the macromolecular configuration landscape as opposed to alteration of the bond scission energy. The scission probability data $p(E)$ can be interpreted within the framework of the TABS model by considering the flow-induced configurational changes to decrease the effective energy barrier to scission. For $\mathrm{We}\gg 1$, the prefactor $g(E)$ can be considered to be independent of E (or We), since the magnitude of tension fluctuation is independent of We in this limit [Fig. 5(b)]. Given this, for $\mathrm{We}\gg 1$, the asymptotic behavior of the scission probability obtained from the simulations can be expressed as $p(E)=\exp(-\Delta E^{*}(E)/kT)$. We note that the data in Fig. 16 can be fitted to this expression

by choosing $\Delta E^* = a/(bE+c)$ where a, b, and c are fitting parameters. In other words, the mechanical stimulus (flow), alters the configurational landscape of the macromolecules, especially in terms of enhancing the probability of finding elongated chains that are more prone to scission. This effect can be quantified and interpreted as a flow-induced reduction in the barrier to scission.

IV. CONCLUSIONS

In this paper, we have presented a novel algorithm for the predictions of flow-induced scission of linear macromolecules in dilute solution. The configurational evolution of the chains as well as the instantaneous segmental tension distribution along the chain backbone are tracked using accurate Brownian dynamics simulations that employ a bead-rod model. The scission criterion is developed based on covalent bond scission force estimates available from the literature and statistical analysis for the instantaneous ST distribution in the bead-rod chains. It is shown that by the use of a normalized ST profile that is independent of the elongation rate E for asymptotically large values of the Weissenberg number, the new algorithm overcomes the inherent time-step dependence present in chain scission simulations that employ instantaneous ST-based criteria to determine scission events.

We have reported results for steady and transient elongational flows and examined the effect of HI on scission in the former, especially in order to probe the origin of the experimentally observed pronounced flow type dependence in the scaling relationships between critical extension rate and sample M_W, i.e., $E_c \propto M_w^{-2}$ in steady elongational flow versus M_w^{-1} in transient flows. Simulation results for steady elongational flow predict $E_c \propto M_w^{-2}$. Moreover, for $E \approx E_c$, the chains unravel via a coil-to-stretch configurational transition, and, since ST attains its maximum at the midpoint of the chain, the midpoint scission hypothesis (MSH) is valid. This leads to a relatively narrow distribution of daughter chains. However, for $E \gg E_c$, the elongated portions of partially coiled chains could break and MSH is not valid. This results in a relatively broad distribution of daughter chains. Hydrodynamic interactions are shown to slow down the unraveling process leading to an increase in E_c with the scaling $E_c \propto M_w^{-1.7}$. The effect of polymer residence time on E_c is examined by investigating the scission of polymer chains that traverse the centerline of a regularized contraction flow. It is found that the scaling relationship between E_c and M_w remains the same as that for steady elongational flow given that the residence time exceeds 5% of the longest relaxation time of the chain. This result suggests that the inverse proportionality of E_c to M_w observed experimentally in contraction flows could be contributed by a number of factors including preshearing effects, potential scission in shear flow at sufficiently large *We* values, i.e., the chain could unravel completely before a tumbling event occurs as suggested by our preliminary investigations [Sim *et al.* (2005)], and/or polydispersity.

ACKNOWLEDGMENTS

This work was supported in part by the Donors of the Petroleum Research Fund administered by the ACS through Grant 36098-AC9, DARPA (Grant 29773A) and the NSF (CTS-0132730). The authors would like to thank Professors Ronald Larson, Jay Schieber, and Patrick Doyle, for their useful discussions.

References

Agarwal, U. S., and R. A. Mashelkar, "Hydrodynamics shielding induced stability of zipping macromolecules in elongational flows," J. Chem. Phys. **100**, 6055–6061 (1994).

Bell, G. I., "Models for the specific adhesion of cells to cells," Science **200**, 618–627 (1978).

Bestul, A. B., "Kinetics of capillary shear degradation in concentrated polymer solutions," J. Chem. Phys. **24**, 1196–1209 (1956).

Bird, R. B., C. F. Curtiss, R. C. Armstrong, and O. Hassager, *Dynamics of Polymeric Liquids, Vol. 2, Kinetic Theory* (Wiley, New York, 1987).

Buchholz, B. A., J. M. Zahn, M. Kenward, G. W. Slater, and A. E. Barron, "Flow-induced chain scission as a physical route to narrowly distributed, high molar mass polymers," Polymer **45**, 1223–1234 (2004).

Choi, H. J., S. T. Lim, P.-Y. Lai, and C. K. Chan, "Turbulent drag reduction and degradation of DNA," Phys. Rev. Lett. **89**, 088302 (2002).

Doyle, P. S., E. S. G. Shaqfeh, and A. P. Gast, "Dynamic simulation of freely draining flexible polymers in steady linear flows," J. Fluid Mech. **334**, 251–291 (1997).

Doyle, P. S., and E. S. G. Shaqfeh, "Dynamic simulation of freely-draining, flexible bead-rod chains: Start-up of extensional and shear flow," J. Non-Newtonian Fluid Mech. **76**, 43–78 (1998).

Evans, E., and K. Ritchie, "Dynamic strength of molecular adhesion bonds", Biophys. J. **72**, 1541–1555 (1997).

Gardiner, C. W., *Handbook of Stochastic Methods* (Berlin, Springer, 1985).

Grandbois, M., M. Beyer, M. Rief, H. Clausen-Schaumann, and H. Gaub, "How strong is a covalent bond?," Science **283**, 1727–1730 (1999).

Horn, A. F., and E. W. Merrill, "Midpoint scission of macromolecules in dilute solution in turbulent flow," Nature (London) **312**, 140–141 (1984).

Hsieh, C.-C., S. J. Park, and R. G. Larson, "Brownian dynamics modeling of flow-induced birefringence and chain scission in dilute polymer solutions in a planar cross-slot flow," Macromolecules **38**, 1456–1468 (2005).

Hunston, D. L., and J. L. Zakin, "Effects of flow-assisted degradation on the drag reduction phenomenon," Polym. Prepr. (Am. Chem. Soc. Div. Polym. Chem.) **19**, 430–438 (1978).

Hur, J. S., E. S. G. Shaqfeh, and R. G. Larson, "Brownian dynamics simulations of single DNA molecules in shear flow," J. Rheol. **44**, 713–742 (2000).

Hur, J. S., E. S. G. Shaqfeh, H. P. Babcock, D. E. Smith, and S. Chu, "Dynamics of dilute and semidilute DNA solutions in the start-up of shear flow," J. Rheol. **45**, 421–450 (2001).

Keller, A., and J. A. Odell, "The extensibility of macromolecules in solution; a new focus for macromolecular science," Colloid Polym. Sci. **263**, 181–201 (1985).

Knudsen, K. D., J. G. Hernández Cifre, J. J. Lopez Cascales, and J. Garcia de la Torre, "Simulation of fracture of flexible polymer chains in transient elongational flow," Macromolecules **28**, 4660–4664 (1995).

Knudsen, K. D., J. G. Hernández Cifre, and J. Garcia de la Torre, "Conformation and fracture of polystyrene chains in extensional flow studied by numerical simulation," Macromolecules **29**, 3603–3610 (1996).

Larson, R. G., H. Hu, D. E. Smith, and S. Chu, "Brownian dynamics simulations of a DNA molecule in an extensional flow field," J. Rheol. **43**, 267–304 (1999).

Lengsfeld, C. S., and T. J. Anchordoquy, "Shear-induced degradation of plasmid DNA," J. Pharm. Sci. **91**, 1581–1589 (2002).

Levy, M. S., I. J. Collins, S. S. Yim, J. M. Ward, N. Titchener-Hooker, P. A. Shamlou, and P. Dunnill, "Effect of shear on plasmid DNA in solution," Bioprocess Eng. **20**, 7–13 (1999).

Lim, S. T., H. J. Choi, S. Y. Lee, J. S. So, and C. K. Chan, "l-DNA induced turbulent drag reduction and its characteristics," Macromolecules **36**, 5348–5354 (2003).

Liu, T. W., "Flexible polymer chain dynamics and rheological properties in steady flows," J. Chem. Phys. **90**, 5826–5843 (1989).

Lopez Cascales, J. J., and J. Garcia de la Torre, "Simulation of polymer chains in elongational flow. Steady-state properties and chain fracture," J. Chem. Phys. **95**, 9384–9392 (1991).

Lopez Cascales, J. J., and J. Garcia de la Torre, "Simulation of polymer chains in elongational flow. Kinetics of chain fracture and fragment distribution," J. Chem. Phys. **97**, 4549–4554 (1992).

Lumley, J. L., "Drag reduction by additives," Annu. Rev. Fluid Mech. **1**, 367–384 (1969).

Matthys, E. F., "Heat transfer, drag reduction, and fluid characterization for turbulent flow of polymer solutions: recent results and research needs," J. Non-Newtonian Fluid Mech. **2–3**, 313–342 (1991).

Neelov, I. M., D. B. Adolf, A. V. Lyulin, and G. R. Davies, "Brownian dynamics simulation of linear polymers under elongational flow: Bead–rod model with hydrodynamic interactions," J. Chem. Phys. **117**, 4030–4041 (2002).

Nguyen, T. Q., and H. H. Kausch, "Chain scission in transient extensional flow kinetics and molecular weight dependence," J. Non-Newtonian Fluid Mech. **30**, 125–140 (1988).

Nguyen, T. Q., and H. H. Kausch, "Effects of solvent viscosity on polystyrene degradation in transient elongational flow," Macromolecules **23**, 5137–5145 (1990).

Odell, J. A., and A. Keller, "Flow-induced chain fracture of isolated linear macromolecules in solution," J. Polym. Sci., Polym. Phys. Ed. **24**, 1889–1916 (1986).

Odell, J. A., A. Keller, and Y. Rabin, "Flow-induced scission of isolated macromolecules," J. Chem. Phys. **88**, 4022–4028 (1988).

Öttinger, H. C., "Brownian dynamics of rigid polymer chains with hydrodynamic interactions," Phys. Rev. E **50**, 2696–2701 (1994).

Öttinger, H. C., *Stochastic Processes in Polymeric Fluids* (Berlin, Springer, 1996).

Perkins, T. T., D. E. Smith, and S. Chu, "Single Polymer Dynamics in an Elongational Flow," Science **276**, 2016–2020 (1997).

Rabin, Y., "Polymer fracture in steady and transient elongational flow," J. Chem. Phys. **86**, 5215–5216 (1987).

Rabin, Y., "On the mechanism of stretching and breaking of polymers in elongational flows," J. Non-Newtonian Fluid Mech. **30**, 119–123 (1988).

Reese, H. R., and B. H. Zimm, "Fracture of polymer chains in extensional flow: Experiments with DNA, and a molecular-dynamics simulation," J. Chem. Phys. **92**, 2650–2662 (1990).

Ryskin, G., "Calculation of the effect of polymer additive in a converging flow," J. Fluid Mech. **178**, 423–440 (1987).

Schieber, J. D., and O. Obasanjo, "On estimating stress in free-draining Kramers chain simulations using stochastic filtering," J. Non-Newtonian Fluid Mech. **127**, 89–93 (2005).

Sim, H. G., R. Sureshkumar, and B. Khomami, "Simulation of polymer chain scission using Kramers model," presented at the 77th Annual Meeting of the Society of Rheology, October 16–20, Vancouver, Canada (2005).

Smith, D. E., and S. Chu, "Response of flexible polymers to a sudden elongational flow," Science **281**, 1335–1340 (1998).

Smith, D. E., H. P. Babcock, and S. Chu, "Single-polymer dynamics in steady shear flow," Science **283**, 1724–1727 (1999).

Somasi, M., B. Khomami, N. J. Woo, J. S. Hur, and E. S. G. Shaqfeh, "Brownian dynamics simulations of bead-rod and bead-spring chains: Numerical algorithms and coarse-graining issues," J. Non-Newtonian Fluid Mech. **108**, 227–255 (2002).

Sureshkumar, R., A. N. Beris, and R. A. Handler, "Direct numerical simulation of the turbulent channel flow of a polymer solution," Phys. Fluids **9**, 743–755 (1997).

Vanapalli, S. A., Ceccio, S. L., and M. J. Solomon, "Universal scaling for polymer chain scission in turbulence," Proc. Natl. Acad. Sci. U.S.A. **103**, 16660–16665 (2006).

Vincent, P. I., "A correlation between critical tensile strength and polymer cross-sectional area," Polymer **13**, 558–604 (1972).

Zhurkov, S. N., and V. E. Korsukov, "Atomic mechanism of fracture of solid polymers," J. Polym. Sci., Polym. Phys. Ed. **12**, 385–398 (1974).

Islam, M., S. A. Vanapalli, and M. J. Solomon, "Inertial effects on polymer chain scission in planar elongational cross-slot flow," Macromolecules **37**, 1023–1030 (2004).